

AD-A098 037 ARMY ARMAMENT RESEARCH AND DEVELOPMENT COMMAND ABERD--ETC F/6 19/4
AN EVALUATION OF THE ALPHA CODE IN ITS ONE-PHASE MODE.(U)
FEB 81 J A SCHMITT, T L MANN

UNCLASSIFIED

ARBRL-NR-03081

SBIE-AD-E430 589

NL

| OF |
40
098047

END
DATE
FEB 81
DTIC

12

LEVEL III

AD-E430589

AD

AD A 098037

MEMORANDUM REPORT ARBRL-MR-03081

AN EVALUATION OF THE ALPHA CODE IN
ITS ONE-PHASE MODE

James A. Schmitt
Thomas L. Mann

February 1981

DTIC
ELECTE
APR 2 2 1981
S B D



US ARMY ARMAMENT RESEARCH AND DEVELOPMENT COMMAND
BALLISTIC RESEARCH LABORATORY
ABERDEEN PROVING GROUND, MARYLAND

Approved for public release; distribution unlimited.

DTIC FILE COPY

81 4 10 009

Destroy this report when it is no longer needed.
Do not return it to the originator.

Secondary distribution of this report by originating
or sponsoring activity is prohibited.

Additional copies of this report may be obtained
from the National Technical Information Service,
U.S. Department of Commerce, Springfield, Virginia
22161.

The findings in this report are not to be construed as
an official Department of the Army position, unless
so designated by other authorized documents.

*The use of trade names or manufacturers' names in this report
does not constitute endorsement of any commercial product.*

UNCLASSIFIED

SECURITY CLASSIFICATION OF THIS PAGE (When Data Entered)

REPORT DOCUMENTATION PAGE		READ INSTRUCTIONS BEFORE COMPLETING FORM
1. REPORT NUMBER MEMORANDUM REPORT ARBRL-MR-03081	2. GOVT ACCESSION NO.	3. RECIPIENT'S CATALOG NUMBER
4. TITLE (and Subtitle) An Evaluation of the ALPHA Code in Its One-Phase Mode	5. TYPE OF REPORT & PERIOD COVERED Memorandum Report	
	6. PERFORMING ORG. REPORT NUMBER	
7. AUTHOR(s) James A. Schmitt Thomas L. Mann	8. CONTRACT OR GRANT NUMBER(s)	
9. PERFORMING ORGANIZATION NAME AND ADDRESS US Army Ballistic Research Laboratory ATTN: DRDAR-BLP Aberdeen Proving Ground, MD 21005	10. PROGRAM ELEMENT, PROJECT, TASK AREA & WORK UNIT NUMBERS RDT&E 1L161102AH43	
11. CONTROLLING OFFICE NAME AND ADDRESS US Army Armament Research & Development Command US Army Ballistic Research Laboratory ATTN: DRDAR-BL Aberdeen Proving Ground, MD 21005	12. REPORT DATE FEBRUARY 1981	
	13. NUMBER OF PAGES 34	
14. MONITORING AGENCY NAME & ADDRESS (if different from Controlling Office)	15. SECURITY CLASS. (of this report) UNCLASSIFIED	
	15a. DECLASSIFICATION/DOWNGRADING SCHEDULE	
16. DISTRIBUTION STATEMENT (of this Report) Approved for public release, distribution unlimited.		
17. DISTRIBUTION STATEMENT (of the abstract entered in Block 20, if different from Report)		
18. SUPPLEMENTARY NOTES		
19. KEY WORDS (Continue on reverse side if necessary and identify by block number) Interior Ballistics Rarefaction Wave Propagation Computer Code Two-Dimensional Code Lagrange ALPHA Gas Dynamics		
20. ABSTRACT (Continue on reverse side if necessary and identify by block number) d11 The initial validation program for ALPHA, a new, state-of-the-art, transient, two-phase, two-dimensional algorithm for interior ballistics calculations is presented. The verification of the simulation of the ballistic cycle for a simplified gun, the Lagrange gun, is made by comparing the computed results with the analytical solution for the core flow and by testing the consistency of the numerical results. The ALPHA simulation of the two-dimensional, one-phase flow in the Lagrange gun is shown to be more accurate than previous calculations.		

TABLE OF CONTENTS

	Page
LIST OF FIGURES.	5
PREFACE.	7
I. INTRODUCTION	9
II. GOVERNING EQUATIONS AND NUMERICAL METHOD	11
III. ONE-DIMENSIONAL LAGRANGE GUN	13
IV. TWO-DIMENSIONAL LAGRANGE GUN	18
V. CONCLUSIONS.	28
ACKNOWLEDGMENT	31
REFERENCES	32
DISTRIBUTION LIST.	33

SEARCHED	INDEXED	SERIALIZED	FILED
			✓
MAY 1964			
FBI - MEMPHIS			
Dirt			
A			

LIST OF FIGURES

Figure		Page
1	The Love and Pidduck Pressure Profiles for the 150-mm Lagrange Gun (Adapted from Reference 3)	17
2	The ALPHA Pressure Profiles for the 150-mm Lagrange Gun	19
3	Comparison of Pressure Profiles After Rarefaction Wave has been Reflected From the Projectile Base for the 150-mm Lagrange Gun.	20
4	Comparison of the Projectile Base Pressure Histories for the 150-mm Lagrange Gun	21
5	Comparison of the Projectile Velocity Histories for the 150-mm Lagrange Gun	22
6	The Heiser and Hensel Projectile Histories for the 20-mm Lagrange Gun (Adapted from Reference 4)	25
7	The ALPHA Projectile Histories for the 20-mm Lagrange Gun	26
8	Comparison of the Velocity Boundary Layer Thicknesses for the 20-mm Lagrange Gun (Given by ALPHA and by Equation (15)).	27
9	Edited ALPHA Velocity Profile at $t = 2.589$ ms for the 20-mm Lagrange Gun.	29
10	The Heiser and Hensel Velocity Profiles for the 20-mm Lagrange Gun (Adapted from Reference 4)	30

PREFACE

The results described in this report were obtained before May 1980. Since that time, additional information has been received and obtained. For example, new calculations have been obtained from Dr. Heiser from the Abteilung für Ballistik im Ernst-Mach-Institut, Federal Republic of Germany and Dr. Hensel from the Deutsch-Französisches Forschungsinstitut, France. The consequences of utilizing higher order temporal differences have been determined. The effects of the corner singularity on the flow simulation have been quantified. These results will be communicated in the BRL technical reports which will supersede this memorandum report.

I. INTRODUCTION

At the ARRADCOM Ballistic Research Laboratory (BRL), a new, state-of-the-art, two-phase, two-dimensional, algorithm, ALPHA, is being developed for interior ballistics under contract to Scientific Research Associates, Inc.¹ ALPHA will simulate the high pressure, turbulent, viscous gas flow and the burning propellant motion behind an accelerating projectile as well as the heat transfer to the gun-tube wall. The consistently split linearized, block, implicit scheme developed by Briley and McDonald² is employed to solve the two-phase, averaged equations.

The validation of the basic models and the numerical technique in an interior ballistics environment is an important and necessary task. As the algorithm is being developed, we at the BRL are testing finished segments for accuracy and are making necessary modifications. By this process, we hope to have a substantial in-house capability with an advanced algorithm when the complete code is delivered. This paper describes aspects of the initial validation program and its findings.

The first phase of the validation program consists of 150-mm and 20-mm Lagrange gun simulations. The Lagrange gun is a perfectly smooth cylindrical tube closed at one end (the breech). The flat-based projectile is initially held fixed at some distance from the breech, and an inert hot gas at high pressure fills the enclosed cavity. The ballistic cycle of the Lagrange gun resembles that of a real gun, if the assumption is made that the propellant burns completely before the projectile moves. The Lagrange gun is used as a benchmark problem to validate the accuracy of simulated wave propagation within the gun tube, the accuracy of the core flow coupling to the projectile motion, the accuracy of the simulated unsteady, viscous, heat-conducting gas flow, and ALPHA's capability to resolve multiple-length scales. A simulation of the two-dimensional flow within the Lagrange gun requires the resolution of several different length scales, for example, those of the core flow, the boundary layer along the gun-tube wall, and the radial flow near the projectile.

Without viscosity, the gas flow in the Lagrange gun is one-dimensional and is determined by propagation of the rarefaction wave. The rarefaction wave is generated by the motion of the projectile and may traverse the distance between the projectile and the breech one or more times before the projectile exits the tube. Under the further assumptions of isentropic

¹H.J. Gibeling, R.C. Buggeln, and H. McDonald, "Development of a Two-Dimensional Implicit Interior Ballistics Code," USA ARRADCOM/Ballistic Research Laboratory Contract Report ARBRL-CR-00411, January 1980, (UNCLASSIFIED). (AD #A084092)

²W.R. Briley and H. McDonald, "Solution of the Multidimensional Compressible Navier-Stokes Equations by a Generalized Implicit Method," *J. Comp. Phys.*, 24, pp 372-397 (1977).

expansion of each element of gas and of constant covolume, Love and Pidduck³ developed an analytic solution for the flow field and projectile motion. Although the formulas for the gas properties become extremely complicated after the rarefaction wave reaches the projectile for the first time, these investigators calculated the gas flow during the complete ballistic cycle for a 150-mm Lagrange gun. If the gas within the gun is viscid, the flow is two-dimensional because of the tube wall boundary layer and the radial flow throughout the flow field. The radial flow is caused by the interaction of the larger gas speed in the axial direction in the core region which governs the projectile motion, and the slower gas speed in the axial direction in the tube wall boundary layer. Because of this disparity in axial velocity in the radial direction, the gas particles in the boundary layer do not keep up with the projectile. Hence, a mass deficit is generated near the corner of the projectile and tube wall. To rectify this deficiency, a radial component of the velocity develops which is toward the tube wall near the projectile. Although no analytic solution exists for the two-dimensional case, a computer simulation of the flow field was calculated by Heiser and Hensel⁴ for a 20-mm gun. They calculated the values of the flow-field variables at the projectile base, the velocity and thermal boundary layers along the tube wall, the radial velocity distribution in the flow, and temperature profiles.

Section II of this report lists the governing equations, states the boundary conditions, and summarizes the numerical procedure used in ALPHA. In Section III, the results of the one-dimensional simulations of the Lagrange gun are given. Using the Love and Pidduck formula for projectile base pressure³, which is valid until the rarefaction wave reaches the projectile, a mesh and time-step resolution study is made and the time-step selection procedures are analyzed. The accuracy of the rarefaction wave propagation and projectile velocity calculations, from the start of projectile motion to time of projectile exit, is determined by comparing them to the Love and Pidduck analytic calculations³ for the 150-mm gun. The two-dimensional ALPHA results for the 20-mm gun are presented in Section IV. Projectile base histories and velocity fields are compared to the predictions of Heiser and Hensel⁴. The 99-percent-velocity boundary-layer thicknesses as a function of time and position as calculated by ALPHA are compared to those which assume a similarity solution. Section V contains the conclusions.

³E.H. Love and F.B. Pidduck, "Lagrange's Ballistic Problem," *Phil. Trans. Roy. Soc.*, 222, pp 167-226, (1921-22).

⁴R. Heiser and D. Hensel, "Calculation of the Axisymmetric Unsteady Compressible Boundary Layer Flow Behind a Moving Projectile," *Proceedings of the Fourth International Symposium on Ballistics*, 1978.

II. GOVERNING EQUATIONS AND NUMERICAL METHOD

The gas flow within the Lagrange gun is assumed to be single phase, compressible, laminar, viscous, heat-conducting, and axisymmetric. The flow is also assumed to obey Stoke's relation of viscosity and Fourier's law of heat conduction. For this case, the governing partial differential equations of Gibelng, et al¹ can be written as:

$$\frac{\partial \rho}{\partial t} + \frac{1}{r} \frac{\partial}{\partial r} (r\rho u) + \frac{\partial}{\partial z} (\rho w) = 0 \quad , \quad (1)$$

$$\begin{aligned} \frac{\partial}{\partial t} (\rho u) + \frac{1}{r} \frac{\partial}{\partial r} (r\rho u^2) + \frac{\partial}{\partial z} (\rho uw) = & - \frac{\partial P}{\partial r} + \frac{\partial}{\partial r} \left[\frac{2}{3} \mu \left(2 \frac{\partial u}{\partial r} - \frac{u}{r} - \frac{\partial w}{\partial z} \right) \right] \\ & + \frac{2\mu}{r} \left(\frac{\partial u}{\partial r} - \frac{u}{r} \right) + \frac{\partial}{\partial z} \left[\mu \left(\frac{\partial u}{\partial z} + \frac{\partial w}{\partial r} \right) \right] , \quad (2) \end{aligned}$$

$$\begin{aligned} \frac{\partial}{\partial t} (\rho w) + \frac{1}{r} \frac{\partial}{\partial r} (r\rho uw) + \frac{\partial}{\partial z} (\rho w^2) = & - \frac{\partial P}{\partial z} + \frac{1}{r} \frac{\partial}{\partial r} \left[\mu r \left(\frac{\partial w}{\partial r} + \frac{\partial u}{\partial z} \right) \right] \\ & + \frac{\partial}{\partial z} \left[\frac{2}{3} \mu \left(2 \frac{\partial w}{\partial z} - \frac{\partial u}{\partial r} - \frac{u}{r} \right) \right] , \quad (3) \end{aligned}$$

$$\begin{aligned} \frac{\partial}{\partial t} (\rho h) - \frac{\partial P}{\partial t} + \frac{1}{r} \frac{\partial}{\partial r} (r\rho uh) + \frac{\partial}{\partial z} (\rho wh) = & u \frac{\partial P}{\partial r} + w \frac{\partial P}{\partial z} - \phi \\ & - \frac{1}{r} \frac{\partial}{\partial r} (rq_r) - \frac{\partial}{\partial z} (q_z) \quad , \quad (4) \end{aligned}$$

where t , r , z , ρ , u , w , P , μ , h , ϕ , q_r , and q_z are the time, radial coordinate, axial coordinate, density, radial velocity, axial velocity, pressure, viscosity coefficient, specific enthalpy, dissipation function, radial component of the heat flux vector, and the axial component of the heat flux vector, respectively. The following algebraic relations are coupled with Eqs. (1) through (4):

$$P = \frac{\rho RT}{M(1-\eta\rho)} \quad , \quad (\text{Noble-Abel equation of state}) \quad (5)$$

$$h = c_v T + P/\rho \quad , \quad (6)$$

$$\mu = c_1 T^{3/2} / (c_2 + T) , \quad (\text{Sutherland's viscosity law}) \quad (7)$$

$$\text{Pr} = 4\gamma / (9\gamma - 5) , \quad (\text{Eucken formula}) \quad (8)$$

$$k = c_p \mu / \text{Pr} , \quad (9)$$

$$(q_r, q_z) = (-k\partial T/\partial r, -k\partial T/\partial z) , \quad (10)$$

where R is the universal gas constant, T is the gas temperature, M is the molar mass, η is the covolume, c_v and c_p are the specific heats, γ is the ratio of specific heats, Pr is the Prandtl number, and k is the coefficient of thermal conductivity. In the simulations, the values of the constants M , c_1 , and c_2 are those used by Heiser and Hensel⁴: $M = 23.8$ g/mole, $c_1 = 1.458 \times 10^{-6}$ kg/(s.m.K^{1/2}), and $c_2 = 110.33$ K. The dissipation function ϕ is defined by

$$\begin{aligned} \phi = & \frac{2}{3} \mu \left[\frac{1}{r} \frac{\partial}{\partial r} (ru) + \frac{\partial w}{\partial z} \right]^2 - 2 \mu \left[\left(\frac{\partial u}{\partial r} \right)^2 + \left(\frac{u}{r} \right)^2 + \left(\frac{\partial w}{\partial z} \right)^2 \right] \\ & - \mu \left[\frac{\partial u}{\partial z} + \frac{\partial w}{\partial r} \right]^2 . \end{aligned} \quad (11)$$

The motion of the projectile is assumed frictionless and is governed by the equation

$$m_p \frac{dw_p}{dt} = 2\pi \int_0^{R^*} P(r, z_p, t) r dr , \quad (12)$$

where R^* is one-half the gun caliber, and m_p , z_p , and w_p are the mass, position, and axial velocity of the projectile, respectively. The gas properties and gun parameters that are not listed above vary with the simulation and are given in Table 1.

The boundary conditions at the breech and projectile are the same for all the simulations, i.e., no-slip, adiabatic walls. The boundary conditions along the centerline are the symmetric conditions; $u = 0$, $\partial w/\partial r = 0$, $\partial T/\partial r = 0$, $\partial \rho/\partial r = 0$. Along the tube wall, the conditions vary according to the simulation and are given in the appropriate section. The density at a no-slip wall is determined by the normal momentum equation at the wall. Because the mesh lines lie on the computational boundaries, one-sided differences are used to approximate the analytic derivative boundary conditions. The initial conditions for each simulation are given in Table 1.

TABLE 1. GEOMETRY AND GAS PROPERTIES FOR THE 150-mm AND 20-mm LAGRANGE GUN SIMULATIONS

150 mm	Bore Diameter	20 mm
1.698 m	Combustion Chamber Length	.175 m
6.0 m	Maximum Travel of Projectile	1.115 m
50 kg	Projectile Mass	.120 kg
$1.0 \times 10^{-3} \text{ m}^3/\text{kg}$	Covolume	$1.08 \times 10^{-3} \text{ m}^3/\text{kg}$
1.222	Gamma	1.271
621.09 MPa	Initial Pressure	300 MPa
2666.8 K	Initial Temperature	3000 K

The Eqs. (1) through (4) are solved numerically by the Briley and McDonald split, linearized, block, implicit scheme.² All the ALPHA calculations are performed using a fully implicit time-step (backward difference) and centered spatial differences. In the ALPHA algorithm, certain terms in the governing equations can be lagged by one time-step in order to simplify the implementation of the algorithm and to enhance its efficiency. The viscosity coefficient μ , the dissipation function Φ all mixed second-order partial derivatives, and the coefficient of thermal conductivity k are lagged in these simulations. The computational mesh in the axial direction is an accordian-type mesh; i.e., the first and last axial grid points are attached to the breech and projectile, respectively, and the mesh expands as the projectile accelerates down the gun tube. The details of the computational mesh for each simulation are given in the appropriate section.

Because the boundaries of the Lagrange gun are assumed adiabatic, the total energy within the computational domain should remain constant throughout a simulation. A conservation test for mass and total energy is incorporated into ALPHA. The deviation of these quantities from their initial values is monitored throughout the calculations.

III. ONE-DIMENSIONAL LAGRANGE GUN

The geometry and gas properties for the 20-mm and 150-mm gun simulations are listed in Table 1. For the one-dimensional calculation, the computational domain (the inclosed cavity behind the projectile) is divided uniformly by four mesh points in the radial direction, and uniformly in the axial direction. Along the tube wall, symmetry boundary conditions are stipulated. Although gas in the simulations is viscous,

the symmetry condition at the wall prevents a boundary layer from forming and the flow is one-dimensional. A measure of the viscous effects in this flow is the deviation of the pressure P and density ρ from the isentropic relation

$$P \left(\frac{1}{\rho} - \eta \right)^{\gamma} = P_0 \left(\frac{1}{\rho_0} - \eta \right)^{\gamma} , \quad (13)$$

where the subscript zero denotes the initial values. In every one-dimensional calculation, the deviation of the left hand side of Eq. (13) is less than 1.4 percent from the right hand side. Hence, the viscous effects of the gas are believed to be negligible, and the ALPHA simulations represent the Love and Pidduck case.³

Because the Briley and McDonald² scheme is implicit, the time-step selection is not coupled to the spatial mesh. Consequently, both the mesh and time-step must be chosen by the user. A study of mesh and time-step refinement reveals the controlling truncation error mechanism. The calculations simulate the propagation of the rarefaction wave to the breech, the reflection of the wave, and its return to the projectile base. Because the pressure is a significant flow variable in a ballistic cycle, we compare the computed pressure value to the analytic value of Love and Pidduck³ at the first time the rarefaction wave returns to the projectile ($t = .24201$ ms). The largest difference between the pressure values occurs at this time and is listed in Table 2. The tabulated results show that for the 10- μ s and 5- μ s time-step runs, the time truncation error dominates the spatial truncation error and that only for sufficiently small time-steps does a mesh refinement increase the accuracy. If the projectile exit times are of the order of ten milliseconds, a constant time-step of the order of microseconds would cause a very lengthy calculation. To increase the accuracy of the results in Table 2 as well as the algorithm's efficiency, higher-order temporal finite differencing should be employed.

TABLE 2. REFINEMENT OF MESH AND TIME-STEP FOR THE ONE-DIMENSIONAL 20-mm LAGRANGE GUN

Constant Time-Step (μ s)	% Deviation*	
	11 Axial Mesh ($\Delta z_0 = 17.50$ mm)	22 Axial Mesh ($\Delta z_0 = 8.33$ mm)
10	2.82	2.80
5	2.09	2.04
2.5	1.59	1.49
1.25	1.39	1.13

* In base pressure values between solutions of Love and Pidduck³ and ALPHA at $t = .24201$ ms.

Initially, ALPHA had two time-step selection procedures for transient calculations - a constant time-step and a variable time-step based on the maximum relative percent change in the velocity components and density. For the runs recorded in Table 3, the variable time-step was increased by 25 percent if the maximum change was less than 4 percent, was decreased by 20 percent if the maximum change was greater than 6 percent, and was not altered if the maximum change was between 4 percent and 6 percent. A comparison of the accuracy and efficiency of time-step selection procedure is given in Table 3. Consider the 22 axial mesh run with the initial time-step $\Delta t_0 = 1.25 \mu s$. The computational work column indicates that the selection procedure for the variable time-step increases the Δt , because the computational work for the variable time-step is less than that for the constant time-step. In fact, the maximum Δt for this case is $10 \mu s$. Comparing the accuracy of this run with the $\Delta t_0 = 10 \mu s$ run, we see only a 8.4 percent increase in accuracy while the initial time-steps differed by a factor of 8. Consequently, a significantly smaller initial time-step for the variable time-step selection procedure does not insure a comparably more accurate solution at the final time. Furthermore, this selection procedure is inefficient. For example, in the case above 84 percent, more computational work was expended with only a 8.4 percent increase in accuracy. The same behavior can also be seen for the 11 axial mesh run. Thus, for time-step refinement, which is important in the validation of computer results, this procedure is unacceptable for this class of problems.

TABLE 3. A COMPARISON OF SELECTION PROCEDURES FOR VARIABLE AND CONSTANT TIME-STEP FOR THE ONE-DIMENSIONAL 20-mm LAGRANGE GUN

Axial Uniform Mesh	Initial Time-Step Δt_0 (μs)	Percent Deviation ^a		Relative Computational Work ^b	
		Variable ($\Delta t_{max} = 10 \mu s$)	Constant	Variable	Constant
22 ($\Delta z_0 = 8.33$ mm)	10	2.14	2.80	3.8	1.7
22	5	2.04	2.04	4.7	3.3
22	1.25	1.96	1.13	7.0	13.2
11 ($\Delta z_0 = 17.50$ mm)	10	2.25	2.82	2.1	1
11	1.25	2.08	1.39	3.8	7.8

^aIn base pressure values between solutions of Love and Pidduck³ and ALPHA at $t = .24201$ ms.

^bNumber of finite difference nodes evaluated to reach $t = .24201$ ms.

Questions on the optimal choice of mesh, time-step, and time-step selection procedure are not addressed. However, it is clear from Table 3 that, for a comparable amount of computational effort, the accuracy can vary substantially depending on the mesh and time-step selection procedure. For example, the calculation with an 11 mesh and a constant time-step of 1.25 μ s takes only 11 percent more computational work than calculation with the 22 mesh and variable time-step ($\Delta t_0 = 1.25 \mu$ s), and yet the accuracy is 29 percent better.

Because neither of the existing time-step selection procedures produces a sufficiently accurate result with good efficiency, a new selection procedure was developed. The axial propagation of the rarefaction wave within the gun tube governs the entire flow field. Thus, a time-step based on the wave speed and the axial computational mesh can be utilized, i.e.,

$$\Delta t = \sigma \cdot \frac{\Delta z_{\max}}{(a+w)_p}, \quad (14)$$

where $(a+w)_p$ is the sound speed plus the gas axial velocity at the projectile base and σ is an input constant. This axial Courant-Friedrichs-Lewy type of condition is not used for reasons of numerical stability but as a compromise time-step selection procedure because it allows sufficiently accurate results in acceptable run times. In the initial phase of the simulation, the axial mesh size and the quantity $(a+w)_p$ do not change significantly; thus, Eq. (14) approximates a constant time-step. In the final phase, the mesh size increases by a factor of 4 or 5 and a time-step selection based on Eq. (14) allows a larger time-step as the spatial truncation error also increases. This time-step selection attempts to preserve some of the accuracy of a constant time-step while allowing a faster calculation. Furthermore, the objection of the selection procedure for the variable time-step is eliminated because a smaller value of the constant σ consistently makes the time-step smaller for a given mesh and improves the accuracy of the calculation.

For the simulation of the one-dimensional 150-mm gun, a uniform axial mesh with 89 grid points is used and the constant σ is set to one. Figure 1 shows the Love and Pidduck pressure decrease due to propagation of the rarefaction wave. The displacement of the projectile and subsequent gas expansion causes the rarefaction wave. At $t = 0$, the pressure is at its initial value. At $t = 0.477$ ms, the position of the rarefaction wave (given by the slope discontinuity) is midway between the projectile and breech. At $t = 0.954$ ms, the rarefaction wave reaches the breech where it is reflected. This wave arrives back at the displaced projectile at $t = 2.117$ ms. The rarefaction wave is again reflected and the entire process is repeated. At projectile exit time $t = 10.58$ ms, the rarefaction wave is approximately halfway to the breech for the third time.

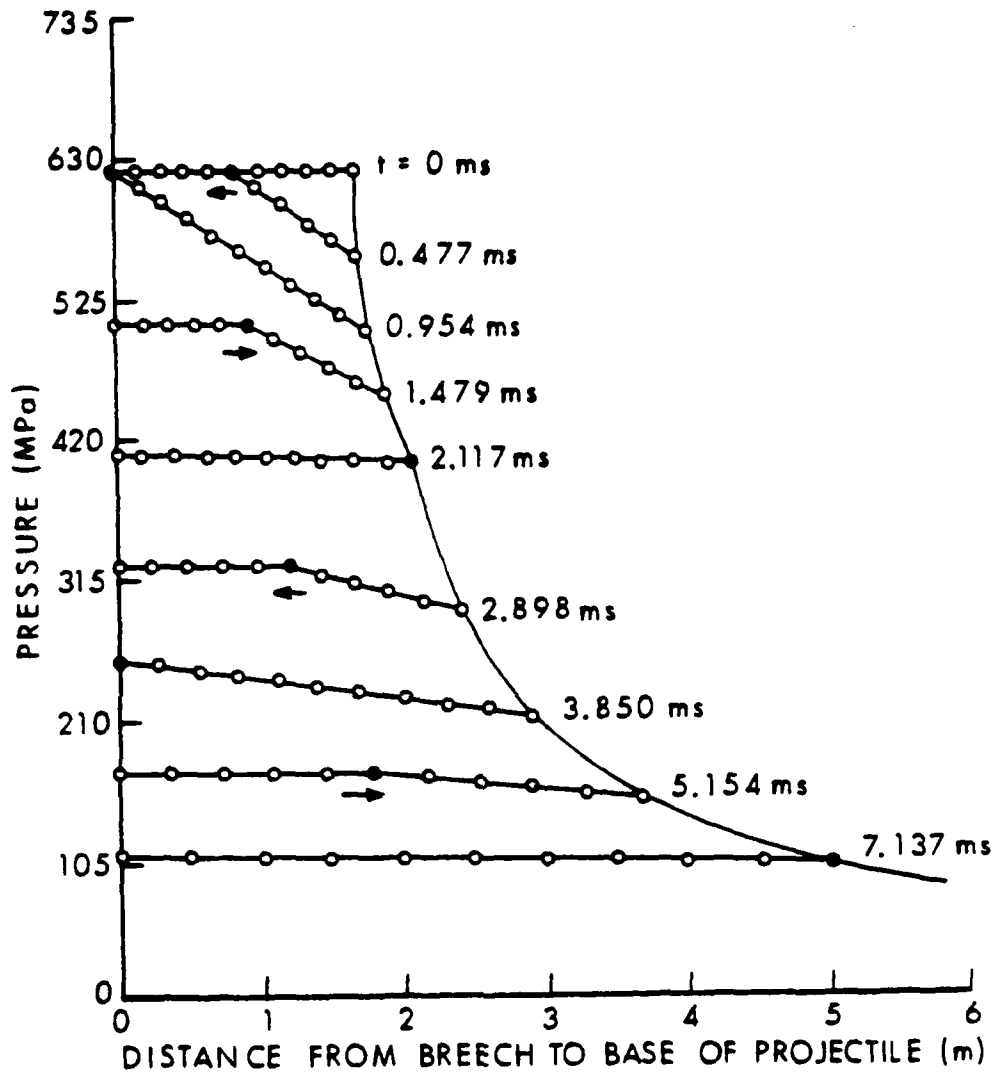


Figure 1. The Love and Pidduck Pressure Profiles for the 150-mm Lagrange Gun (Adapted from Reference 3)

The magnitude in the slope discontinuity of the pressure curve decreases with time due to the equilibration of the pressures during the gas expansion. The position curve of the projectile shows a distinct slope discontinuity when the rarefaction wave reaches the projectile for the first time. At the second arrival $t = 7.137$ ms, the magnitude of the slope discontinuity is extremely small and cannot be discerned in Figure 1. The ALPHA results are plotted in Figure 2. Although the times at which the pressure profiles are plotted do not coincide with those of Love and Pidduck, the same features seen in Figure 1 are present in Figure 2.

Figure 3 shows a detailed comparison of the Love and Pidduck pressure profile with the ALPHA pressure profile at $t = 2.898$ ms. At the breech and projectile (away from the rarefaction wave), the difference between the pressure values are less than 0.2 percent. At the rarefaction wave, the difference is less than 1.1 percent. The slope discontinuity in the analytic solution is smeared out in the numerical calculation. The ALPHA pressure history at the projectile is compared with the analytic values in Figure 4. Throughout most of the calculation, the values differ by less than 0.4 percent. The deviation increases to over 2 percent when the rarefaction wave reaches the projectile. This is consistent with results shown in Figure 3; i.e., the accuracy of the pressure value at the rarefaction front is less than at a distance from it. The decrease in the accuracy of the ALPHA pressure values for $t > 6$ ms is due to the increased truncation error generated by the expanding axial mesh. Figure 5 shows the comparison of the velocity histories of the projectile. The ALPHA values are within 0.6 percent of the Love and Pidduck values through projectile exit time.

IV. TWO-DIMENSIONAL LAGRANGE GUN

The no-slip boundary condition along the tube wall is imposed for this calculation, and a two-dimensional flow develops. The tube wall is assumed to be adiabatic. The computational grid at $t = 0$ is given in Table 4. Grid concentrations along the tube wall and projectile are used to resolve the boundary layer and radial flow near the projectile, respectively. Because the mesh lines lie on the computational boundaries, the corner formed by the tube wall and projectile base gives rise to a corner singularity; that is, the axial velocity at the vertex of the corner is not uniquely defined. If the mesh point at the vertex is viewed as part of the tube wall, its axial velocity should be zero. If this mesh point is viewed as part of the projectile, its axial velocity should be the velocity of the projectile. For all calculations reported in this paper, the former is used. No significant difference in the flow field occurs when the latter is chosen.

The time-step procedure for this run is the minimum time-step which is generated by the variable time-step procedure and by Eq. (14). The rationale is based on the facts that the variable time-step procedure has been used to accurately compute compressible boundary layers and

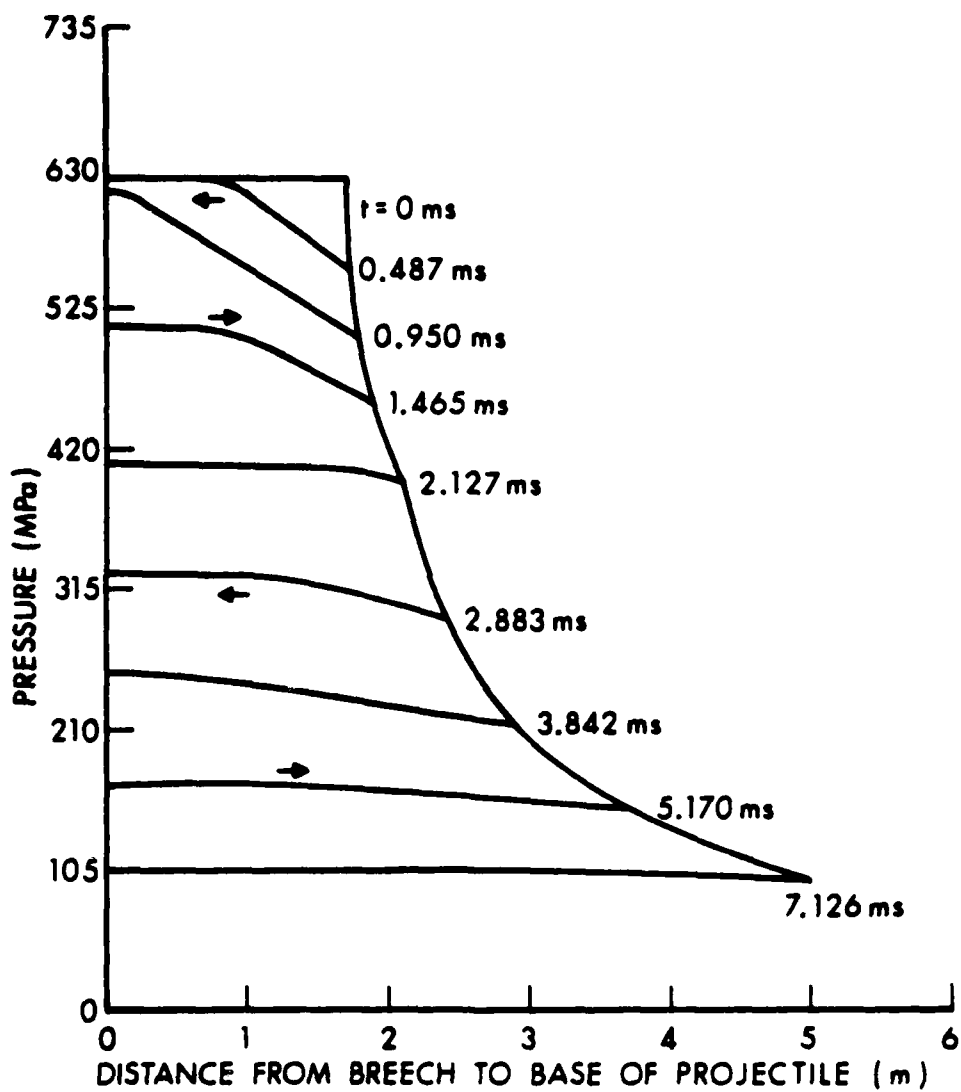


Figure 2. The ALPHA Pressure Profiles for the 150-mm Lagrange Gun

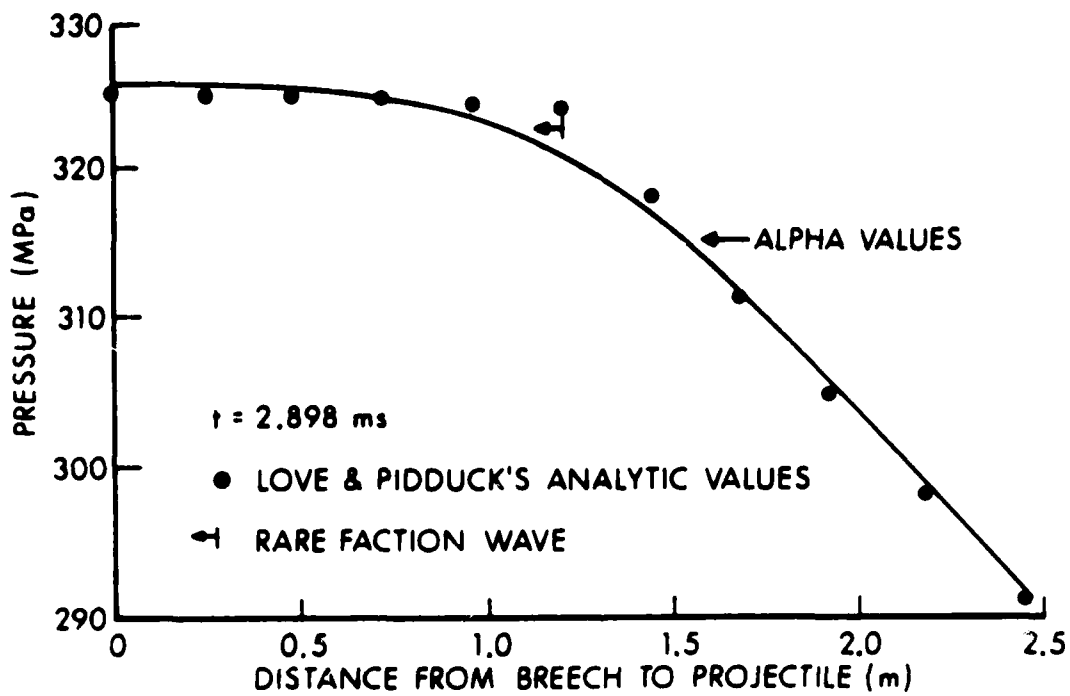


Figure 3. Comparison of Pressure Profiles After Rarefaction Wave Has Been Reflected From the Projectile for the 150-mm Lagrange Gun

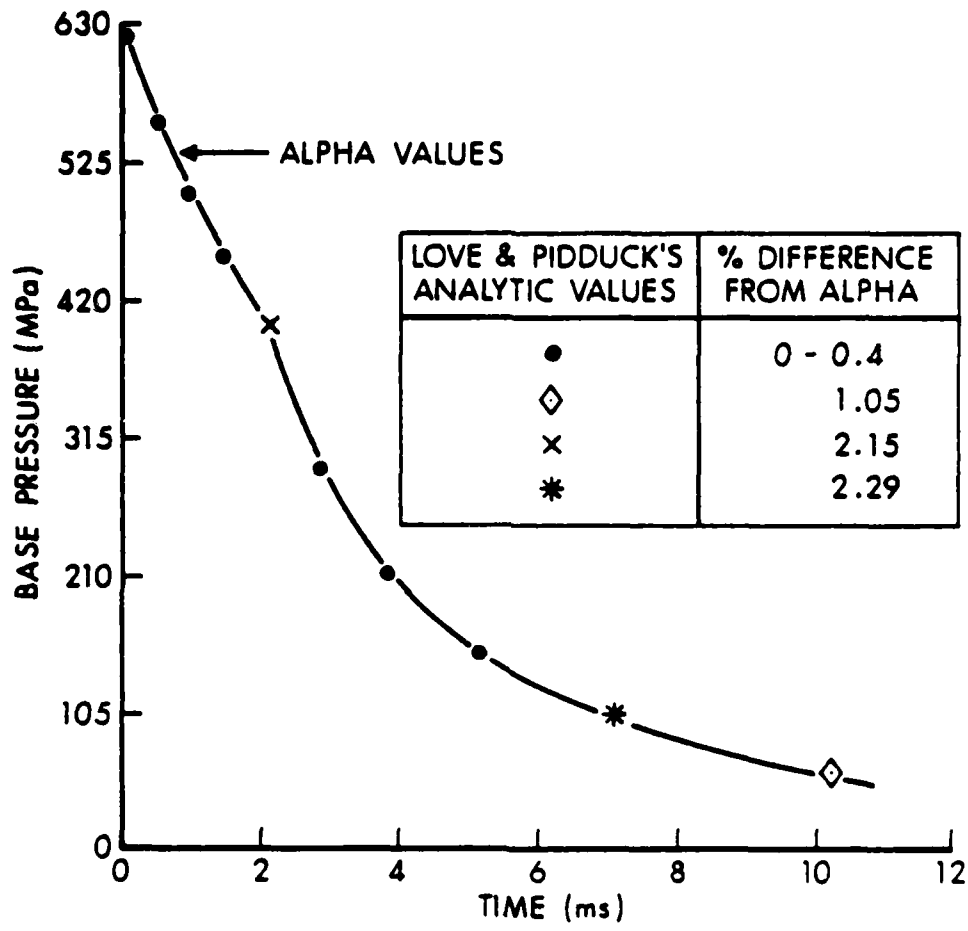


Figure 4. Comparison of the Projectile Base Pressure Histories for the 150-mm Lagrange Gun

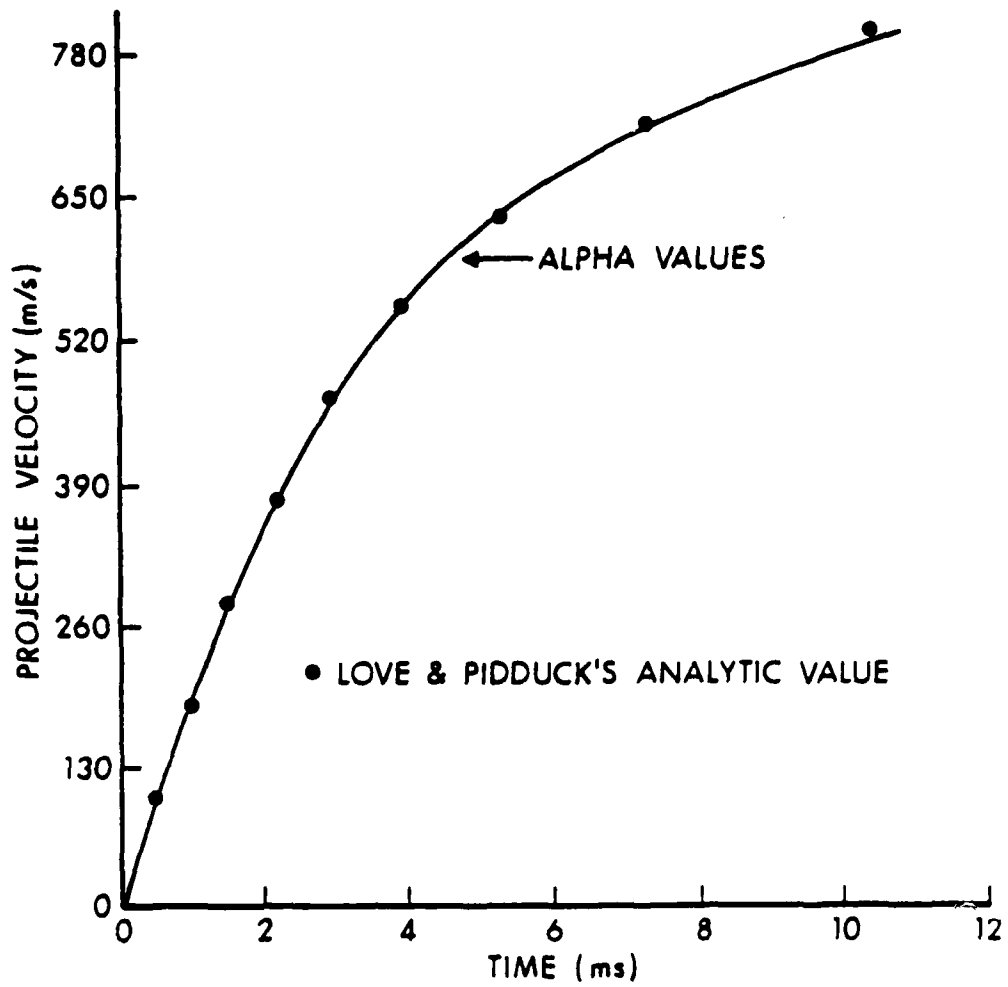


Figure 5. Comparison of the Projectile Velocity Histories for the 150-mm Lagrange Gun

TABLE 4. COMPUTATIONAL MESH FOR THE TWO-DIMENSIONAL
20-mm LAGRANGE GUN SIMULATION

Number	Radial Increments (mm)	Axial Increments (mm)
1	1.95821 (CenterLine)	3.79072 (Breech)
	1.81402	4.67230
	1.56520 (Midway)	5.68545
	1.26983	6.81124
5	.97971	8.00911
	.72696	9.21362
	.52395	10.33597
	.36977	11.27290
10	.25710	11.92313 (Midway)
	.17692	12.20841
	.12087	12.09234
	.08218	11.58988
15	.05568	10.76340
	.03764	9.70698
	.02541	8.52543
	.01713	7.31528
20	.01155	6.15246
	.00778 (Tube Wall)	5.08793
		4.14922
		3.34532
25		2.67246
		2.11928
		1.67080
		1.31119
30		1.02524
		.79940
		.62193
		.48303
35		.37465
		.29029
		.22474
		.17388
40		.13448
		.10395
		.08035
		.06207
45		.04796
		.03704
		.02861
		.02210
45		.01706
		.01318
		.01017
		.00786
45		.00607
		.00468
		.00362
	.00276 (Projectile)	

that the time-step given by Eq. (14) produces at most a 2.3-percent error in pressure values for propagation of the rarefaction wave in the 150-mm gun. By using the minimum, both phenomena which occur in this two-dimensional problem should be accurately computed. For this simulation, the constant σ is set to one.

The gun geometry, gas parameters, initial conditions (see Table 1), and boundary conditions used in the simulation are identical to those used by Heiser and Hensel⁴. Despite this duplicate setup, the computed projectile velocity at the muzzle differ greatly: Heiser and Hensel computed over a 700 m/s value (see Figure 6), while the ALPHA value is less than 600 m/s (see Figure 7). To determine the more accurate calculation, these times were compared with the arrival time of the rarefaction wave at the projectile as determined by Love and Pidduck³. Although the development of the boundary layer along the tube wall may alter somewhat the rarefaction-wave propagation, the arrival times of the rarefaction wave for the one-dimensional and two-dimensional simulations should be comparable. Taking the slope discontinuity in the curves of the pressure history as the arrival time of the rarefaction wave at the projectile, we find that the arrival time computed by Heiser and Hensel is 96 percent larger than the Love and Pidduck value of .24201 ms. The value computed by ALPHA is 4 percent smaller; consequently, we feel that the ALPHA result is more accurate. Because a higher pressure is maintained at the projectile base for a longer time in Heiser and Hensel's simulation, the projectile velocity at the muzzle is larger and the projectile exit time is shorter. The dashed curves in Figure 6 are the Heiser and Hensel results for a breechless gun (the simple wave solution represents the case when the rarefaction wave never returns to the projectile).

The axial velocity near the centerline for a given time can be approximated well by a linear profile with the axial velocity equal to zero at the breech, and equal to the projectile velocity at the projectile base. Furthermore, the gun-tube wall is at rest. This configuration resembles that for the steady Falkner-Skan similarity solution⁵ for the boundary layer with a linear core velocity. The boundary-layer thicknesses away from the projectile base are almost constant as are the boundary-layer thicknesses in the corresponding Falkner-Skan solution. (See Figure 8.) In the similarity solution the boundary-layer thickness is given by

$$\delta = K \left[\frac{\bar{u}z}{\rho v^*} \right]^{1/2}, \quad (15)$$

⁵G.K. Batchelor, *An Introduction to Fluid Dynamics*, Cambridge at the University Press, pp. 316-18, 1970.

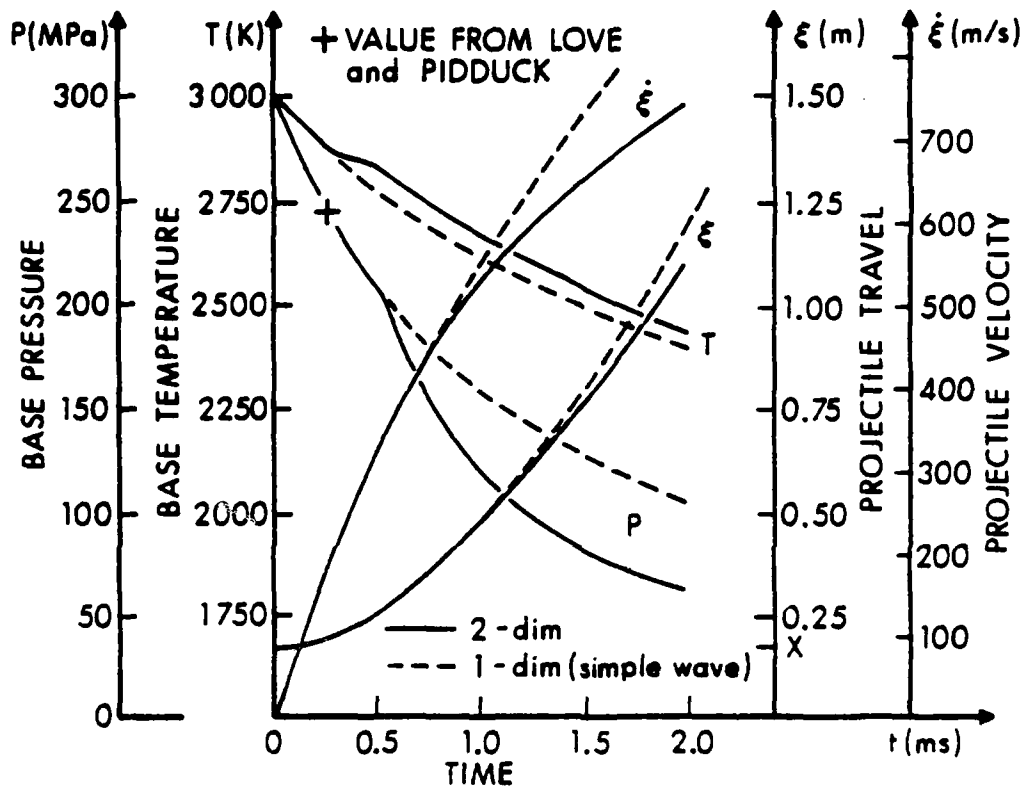


Figure 6. The Heiser and Hensel Projectile Histories for the 20-mm Lagrange Gun (Adapted from Reference 4)

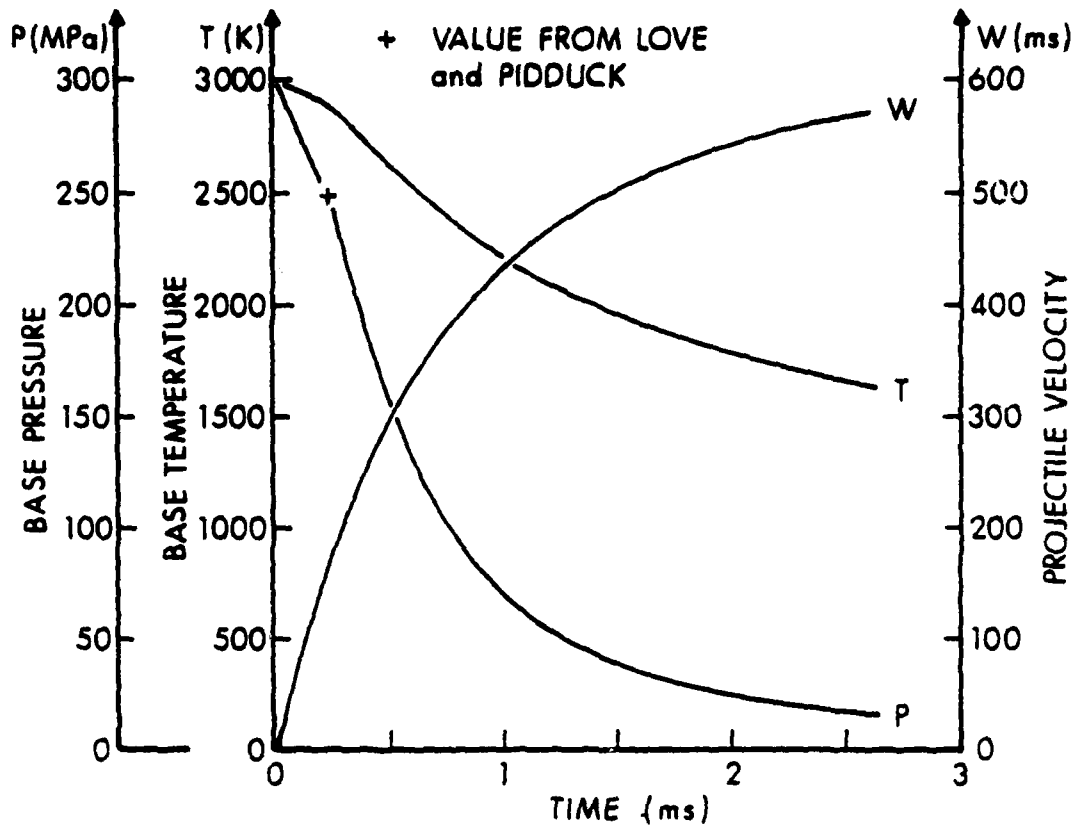


Figure 7. The ALPHA Projectile Histories for the 20-mm Lagrange Gun

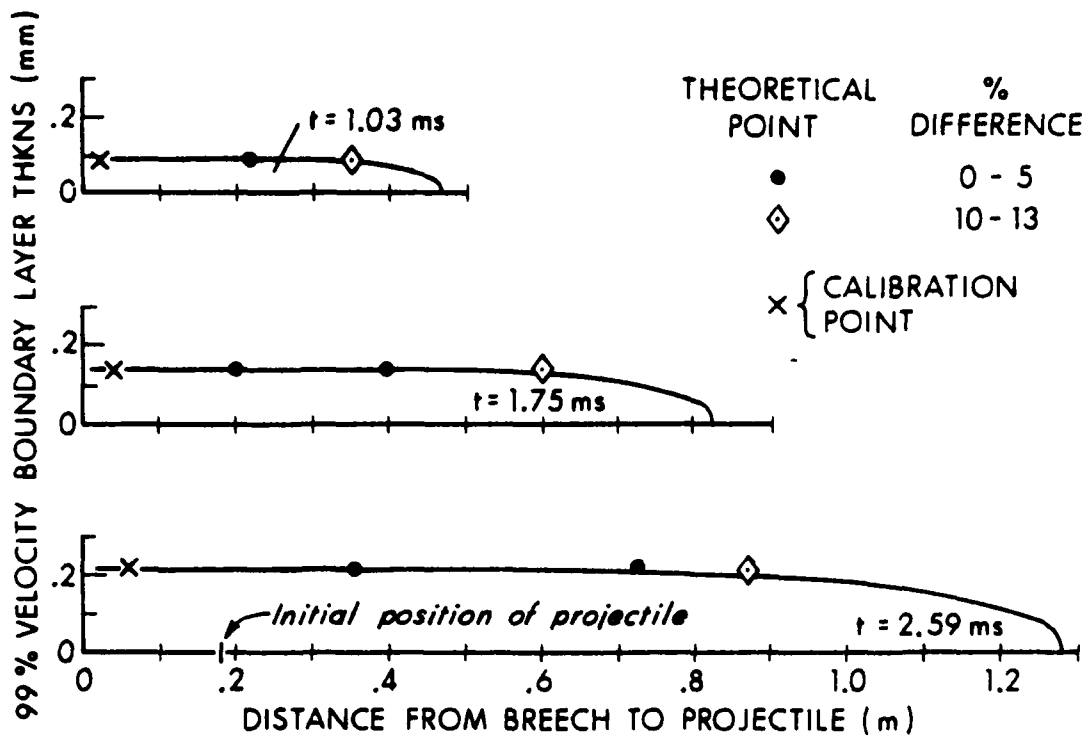


Figure 8. Comparison of the Velocity Boundary Layer Thicknesses for the 20-mm Lagrange Gun (Given by ALPHA and by Equation (15))

where K is a proportionality constant and $\bar{\mu}$, $\bar{\rho}$, z , \bar{w} , are the gas viscosity coefficient, gas density, axial position, and axial gas velocity in the core flow, respectively. The value of the constant K at specific times is computed at a calibration point (the second axial mesh point from the breech) from Eq. (15) by using the core values and the 99-percent-velocity boundary-layer thickness value which is calculated from the ALPHA velocity field. Once the constant K is determined, a "theoretical" value of the boundary-layer thickness via Eq. (15) can be computed for the given time and for any position from the ALPHA centerline values of $\bar{\mu}$, $\bar{\rho}$, and \bar{w} . The comparisons between these "theoretical" values and the actual 99-percent-velocity boundary-layer values are given in Figure 8. Away from the projectile base, these values differ by no more than 5 percent, and the ALPHA values seem to be self-consistent. The boundary-layer thickness is largest at the projectile exit when it reaches 0.22 mm. The thicknesses of the velocity boundary-layer calculated by Heiser and Hensel are less than 0.1 mm. This discrepancy is reasonable because these investigators predicted a larger core velocity, which increases the core Reynolds number and decreases the boundary-layer thickness.

A typical velocity field computed by ALPHA is shown in Figure 9. Because the radial velocity is of the order of 1 m/s and the axial velocity is of the order of 100 m/s, different plotting scales are used. Figure 9 shows only the velocity vectors for a selected number of mesh points. If the velocity vectors at each mesh point were shown, the high concentration of grid points would obscure the flow picture near the wall and projectile. The ALPHA velocity field does not change qualitatively, but only quantitatively in time. The axial flow in the core accelerates from zero at the breech to the projectile velocity. The tube-wall boundary layer can clearly be seen. Figure 9 does not show the small non-zero radial velocity, in the interior of the computational domain and away from the projectile, because their magnitudes are so small. Close to the projectile, the radial flow reverses direction and significantly increases in magnitude. The radial flow is developed in order to rectify the mass deficit at the corner of the projectile base and tube wall caused by the boundary layer along the tube wall. Figure 10 shows Heiser and Hensel's velocity field at two times. Despite the fact that these velocity fields are near projectile exit and are only 0.1 ms apart, they differ significantly in the radial component. The ALPHA velocity field is more consistent with the flow-field mechanisms.

V. CONCLUSIONS

The initial validation program for ALPHA via the Lagrange gun reveals several important facts. (1) Higher-order schemes for temporal finite differencing should be used to increase ALPHA's accuracy and efficiency. (2) A better procedure for time-step selection should be developed for the class of problems involving unsteady wave propagation. (3) Despite a relatively coarse core mesh and large time-step, ALPHA can compute

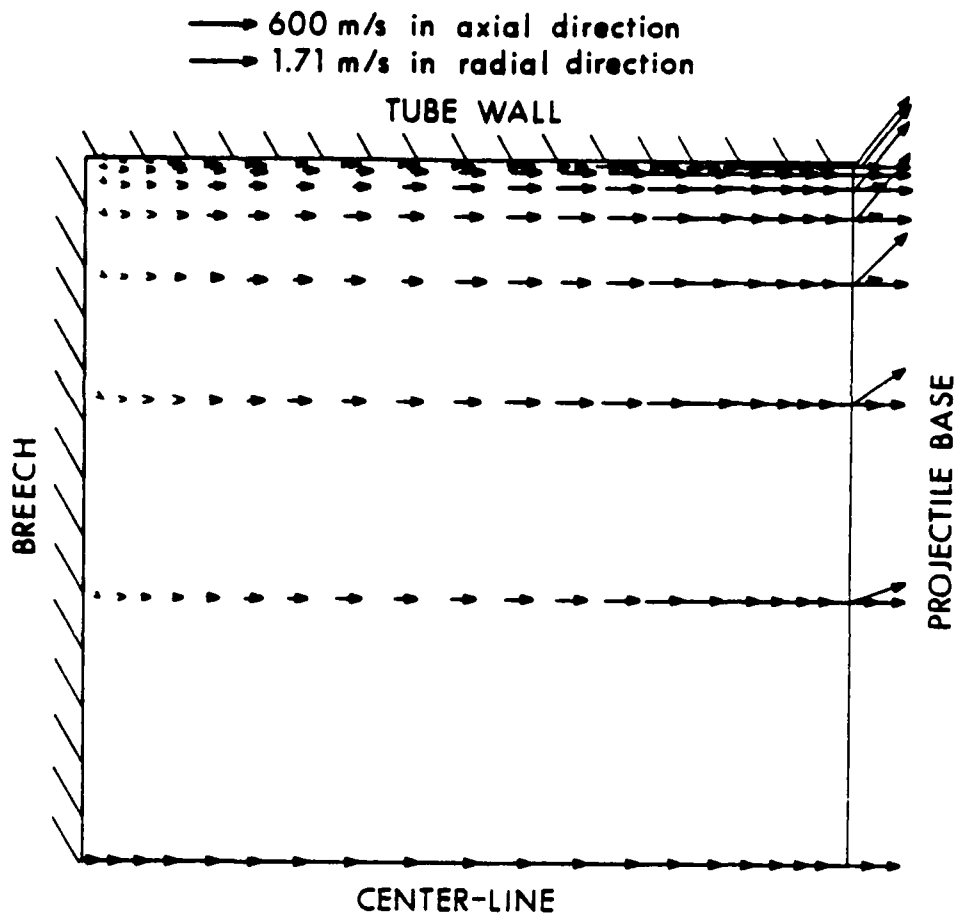


Figure 9. Edited ALPHA Velocity Profile at $t = 2.589$ ms for the 20-mm Lagrange Gun

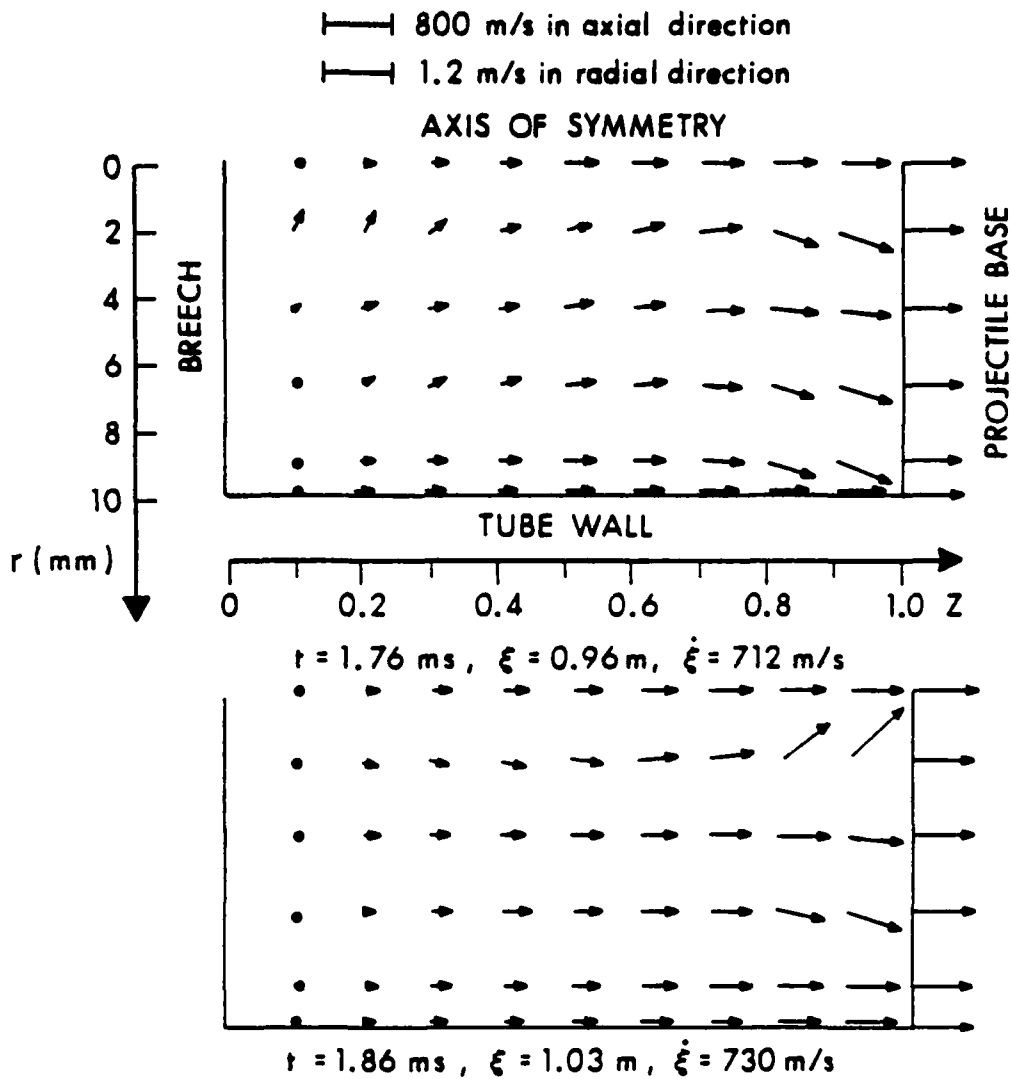


Figure 10. The Heiser and Hensel Velocity Profiles for the 20-mm Lagrange Gun (Adapted from Reference 4)

the propagation of one-dimensional rarefaction waves to within 2.3 percent and projectile motion to within 0.6 percent. (4) ALPHA's simulation of the two-dimensional Lagrange gun is more accurate than previous calculations. (5) The boundary-layer thickness along the gun-tube wall computed by ALPHA is consistent. (6) ALPHA calculations conserve mass and energy to within 0.3 percent for a complete simulation.

The importance of the analytical solution of Love and Pidduck³ in this study cannot be overemphasized. This analytic solution is used, at least partially, in forming four out of the six conclusions above. Furthermore, in the initial validation program of a new code, an analytic solution is superior to experiments because the uncertainties in the experimental set-up and the errors in the measurements are absent.

Future work with ALPHA consists of testing higher-order schemes for temporal finite differences and procedures for time-step selection for the Lagrange gun environment. The radial flow and its effects on the temperature field, especially near the projectile, as well as the effects of the multivalued corner point (at the intersection of the gun-tube wall and projectile base) on the flow field will be studied in detail.

ACKNOWLEDGMENT

The authors have benefited greatly from many discussions of the ALPHA algorithm with Dr. Howard J. Gibeling at Scientific Research Associates, Inc.

REFERENCES

1. H.J. Gibeling, R.C. Buggeln, and H. McDonald, "Development of a Two-Dimensional Implicit Interior Ballistics Code," Contract Report No. ARBRL-CR-00411, USA ARRADCOM/BRL, APG, MD, January 1980. (UNCLASSIFIED) (AD #A084092)
2. W.R. Briley and H. McDonald, "Solution of the Multidimensional Compressible Navier-Stokes Equations by a Generalized Implicit Method," J. Comp. Phys., 24, pp 372-397, 1977.
3. E.H. Love and F.B. Pidduck, "Lagrange's Ballistic Problem," Phil. Trans. Roy. Soc., 222, pp 167-226, 1921-22.
4. R. Heiser and D. Hensel, "Calculation of the Axisymmetric Unsteady Compressible Boundary Layer Flow Behind a Moving Projectile," Proceedings of the Fourth International Symposium on Ballistics, 1978.
5. G.K. Batchelor, An Introduction to Fluid Dynamics, Cambridge at the University Press, pp 316-18, 1970.

DISTRIBUTION LIST

<u>No. of Copies</u>	<u>Organization</u>	<u>No. of Copies</u>	<u>Organization</u>
12	Commander Defense Technical Info Center ATTN: DDC-DDA Cameron Station Alexandria, VA 22314	1	Commander US Army Communications Research and Development Command ATTN: DRDCO-PPA-SA Fort Monmouth, NJ 07703
1	Commander US Army Materiel Development and Readiness Command ATTN: DRCDMD-ST 5001 Eisenhower Avenue Alexandria, VA 22333	1	Commander US Army Electronic Research and Development Command Technical Support Activity ATTN: DELSD-L Fort Monmouth, NJ 07703
2	Commander US Army Armament Research and Development Command ATTN: DRDAR-TSS Dover, NJ 07801	2	Commander US Army Missile Command ATTN: DRSMI-R DRSMI-YDL Redstone Arsenal, AL 35809
1	Commander US Army Armament Materiel Readiness Command ATTN: DRSAR-LEP-L, Tech Lib Rock Island, IL 61299	1	Commander US Army Tank Automotive Research and Development Command ATTN: DRDTA-UL Warren, MI 48090
3	Director USA ARRADCOM/Benet Weapons Lab ATTN: DRDAR-LCB-TL M.N. Hussain J.E. Zweig Watervliet, NY 12189	1	Director US Army TRADOC Systems Analysis Activity ATTN: ATAA-SL, Tech Lib White Sands Missile Range, NM 88002
1	Commander US Army Aviation Research and Development Command P.O. Box 209 St. Louis, MO 61366	2	Commander Naval Surface Weapons Center ATTN: J. East Tech Lib Dahlgren, VA 22448
1	Director US Army Air Mobility Research and Development Laboratory Ames Research Center Moffett Field, CA 94035	1	Commander Naval Weapons Center ATTN: 3431, Tech Lib China Lake, CA 93555

DISTRIBUTION LIST

<u>No. of Copies</u>	<u>Organization</u>	<u>No. of Copies</u>	<u>Organization</u>
2	Commander Naval Ordnance Station ATTN: S.E. Mitchell Tech Lib Indian Head, MD 20640	2	Los Alamos Scientific Lab ATTN: D. Durack B. Wendorff Los Alamos, NM 87545
2	Lawrence Livermore Laboratory University of California ATTN: S.C. Buckingham S-W Kang Livermore, CA 94450	1	University of Illinois-Urbana Mechanics & Industrial Engineering ATTN: S.L. Soo Urbana, IL 61801
1	Paul Gough Associates, Inc. ATTN: P.S. Gough P.O. Box 1614 Portsmouth, NH 03801	1	Massachusetts Institute of Technology Dept. of Material Science and Engineering ATTN: J. Szehely 77 Massachusetts Avenue Cambridge, MA 02139
1	Science Applications, Inc. ATTN: R.B. Edelman 21133 Victory Blvd., Suite 216 Canoga Park, CA 91303	1	Princeton University Guggenheim Laboratories Dept. of Aerospace and Mechanical Science ATTN: L.H. Caveny P.O. Box 710 Princeton, NJ 08540
2	Scientific Research Asso., Inc. ATTN: H. McDonald H. Giebling P.O. Box 498 Glastonbury, CT 06033		<u>Aberdeen Proving Ground</u>
1	Pennsylvania State University Dept. of Mechanical Engineering ATTN: K.K. Kuo University Park, PA 16801		Dir, USAMSAA ATTN: DRXSY-D DRXSY-MP, H. Cohen
1	University of Maryland Institute of Physics Science and Technology ATTN: S.I. Pai College Park, MD 20742		Cdr, USATECOM ATTN: DRSTE-TO-F Dir, USACSL, Bldg. E5515 ATTN: DRDAR-CLB-PA
2	University of Cincinnati ATTN: A. Hamed W. Tabakoff Cincinnati, OH 45221		

USER EVALUATION OF REPORT

Please take a few minutes to answer the questions below; tear out this sheet, fold as indicated, staple or tape closed, and place in the mail. Your comments will provide us with information for improving future reports.

1. BRL Report Number _____

2. Does this report satisfy a need? (Comment on purpose, related project, or other area of interest for which report will be used.)

3. How, specifically, is the report being used? (Information source, design data or procedure, management procedure, source of ideas, etc.) _____

4. Has the information in this report led to any quantitative savings as far as man-hours/contract dollars saved, operating costs avoided, efficiencies achieved, etc.? If so, please elaborate.

5. General Comments (Indicate what you think should be changed to make this report and future reports of this type more responsive to your needs, more usable, improve readability, etc.) _____

6. If you would like to be contacted by the personnel who prepared this report to raise specific questions or discuss the topic, please fill in the following information.

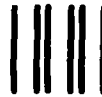
Name: _____

Telephone Number: _____

Organization Address: _____

FOLD HERE

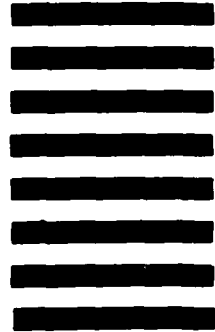
Director
US Army Ballistic Research Laboratory
Aberdeen Proving Ground, MD 21005



NO POSTAGE
NECESSARY
IF MAILED
IN THE
UNITED STATES

OFFICIAL BUSINESS
PENALTY FOR PRIVATE USE, \$300

BUSINESS REPLY MAIL
FIRST CLASS PERMIT NO 12062 WASHINGTON, DC
POSTAGE WILL BE PAID BY DEPARTMENT OF THE ARMY



Director
US Army Ballistic Research Laboratory
ATTN: DRDAR-TSB
Aberdeen Proving Ground, MD 21005

FOLD HERE

DATE
FILMED
-8